Structural Engineering and Mechanics, *Vol. 50, No. 1 (2014) 105-119*
DOI: http://dx.doi.org/10.12989/sem.2014.50.1.105

Movement identification model of port container crane based on structural health monitoring system

Mosbeh R. Kaloop[*1,2], Mohamed A. Sayed[1a], Dookie Kim[1b] and Eunsung Kim[3c]

[1]*Department of Civil and Environmental Engineering, Kunsan National University, Kunsan, South Korea*
[2]*Department of Public Works and Civil Engineering, Mansoura University, Mansoura, Egypt*
[3]*Korea Maintenance Company, Seoul, South Korea*

(Received July 5, 2013, Revised February 14, 2014, Accepted February 15, 2014)

Abstract. This study presents a steel container crane movement analysis and assessment based on structural health monitoring (SHM). The accelerometers are used to monitor the dynamic crane behavior and a 3-D finite element model (FEM) was designed to express the static displacement of the crane under the different load cases. The multi-input single-output nonlinear autoregressive neural network with external input (NNARX) model is used to identify the crane dynamic displacements. The FEM analysis and the identification model are used to investigate the safety and the vibration state of the crane in both time and frequency domains. Moreover, the SHM system is used based on the FEM analysis to assess the crane behavior. The analysis results indicate that: (1) the mean relative dynamic displacement can reveal the relative static movement of structures under environmental load; (2) the environmental load conditions clearly affect the crane deformations in different load cases; (3) the crane deformations are shown within the safe limits under different loads.

Keywords: structural health monitoring; finite element model; neural network; container crane

1. Introduction

The steel container crane structure is the key equipment of the handling operations in the harbor. The behavior of these harbor structures presents several hazards in particular because of the difficult conditions of building and extreme loadings (storms) (Godoy *et al.* 2008). Under the effect of long-term impact loads, the mechanical conditions of the container crane will appear many failures, such as the running failure of the slewing bearing, crack and deformation of the metal structure and others, which posses a grave threat for the safety of devices and operators (Richard *et al.* 2001, Zhiping *et al.* 2011, Ding *et al*. 2012). Environmental and operational variations, such as varying temperature, moisture, and loading conditions affecting the dynamic response of the structures cannot be overlooked either (Sohn *et al*. 2004). In fact, these changes can often mask subtler structural changes caused by damage. Moreover, with the possible climatic

[*]Corresponding author, Research Professor, E-mail: mosbeh.kaloop@gmail.com
[a]Master Student, E-mail: mabdelmonem86@gmail.com
[b]Professor, E-mail: kim2kie@chol.com
[c]General Manager, E-mail: caelumiter@gmail.com

http://www.techno-press.org/?journal=sem&subpage=8 ISSN: 1225-4568 (Print), 1598-6217 (Online)

changes, there is a need to update extreme wind speed and corresponding storm loading on structures with a view to analyze the relative change in safety level (Godoy *et al.* 2008). The process of implementing a movement and damage identification strategy for civil and mechanical engineering infrastructure is referred to Structural Health Monitoring (SHM) (Sohn *et al.* 2004, Kaloop 2012). By SHM of container cranes, the deterioration tendency of metal structure can be predicted and sudden accidents may be avoided.

Crane damage and subsequent downtime has a major impact on indirect losses and post-disaster recovery. Ports have received little attention compared with other infrastructures; however, significant damage to a major port may have a significant impact on the local and national economy (Kosbab *et al.* 2009).

Most building codes and specifications address steel structures members loads and set minimum standards for these loads. The studied crane is a steel container crane that lifts objects by a hoist, which is fitted in a hoist trolley and move horizontally on pair of rails fitted under a beam. The environmental loads (wind speed and ambient temperature) and the container-moving load are the two main loads affecting the crane.

The finite element model (FEM) analysis is often carried out to assist the structure design and limited real analysis. Therefore, the real loading conditions were always much more complicated than the modelers can imagine. Li *et al.* (2006) referred to that the structural response under affecting loads were consists mainly on three components: static, quasi-static and dynamic components. The accelerometer sensor is one of sensors, which are used to measure the dynamic component of structures, whereas they can be used to detect relative higher vibration of structures (Meng *et al.* 2007). In addition, the accelerometer is able to extract acceleration response of a structure with natural frequency up to 1,000 Hz because of the high sampling frequency (Chan *et al*. 2006). Different sensors are also used to measure and investigate the dynamic vibration of structures and maintenance, e.g., Global Positioning System (GPS) (Nickitopoulou *et al.* 2006, Meng *et al.* 2007, Moschas *et al.* 2011); laser scanner (Gikas 2012a); and ground-based microwave interferometry (Gentile 2010, Gikas 2012b).

Dynamic measurements of several high-rise buildings, suspension bridges and offshore structures were undertaken and used in system identification (Hart and Yao 1977, Magalhaes *et al*. 2007). During this period the interest in using parametric time domain models for system identification of structural systems increased. In civil engineering, the use of multivariate time domain models has especially attracted the attention, see (Heij and Schagen 2007, Weng *et al*. 2008, Heo and Jeon 2009). The system models can be simulating the effects of the physical laws pertaining to the system when available with the help of input-output quantities (Erdogan and Gulal 2009). In addition, when there is little information on the physical laws pertaining to the system or when the system is too complex, identification methods such as parametric identification are used to define the model of the system. In this case, preliminary assumptions are made on the order of complexity, input and output parameters of the system. The model is then expressed as the relationship between the selected system inputs and outputs (Gevers *et al.* 2006, Erdogan and Gulal 2009). Erdogan and Gulal (2009), Elnabwy *et al.* (2013), Kaloop and Li (2014) used the model identification based on neural networks to identify the movements of bridges and to estimate the structural movements.

The cranes health monitoring analysis studies are less compared to other different structures studies; refer to (Deng and Xu 2009, Bhimani and Soaderberg 2010, Zhiping *et al*. 2011, Ding *et al*. 2012). The high cost of establishing a SHM system is considered one of the important issues

Fig. 1 Crane collapse by Typhoon in Pusan ports (Gamman, Jasungdae 2003)

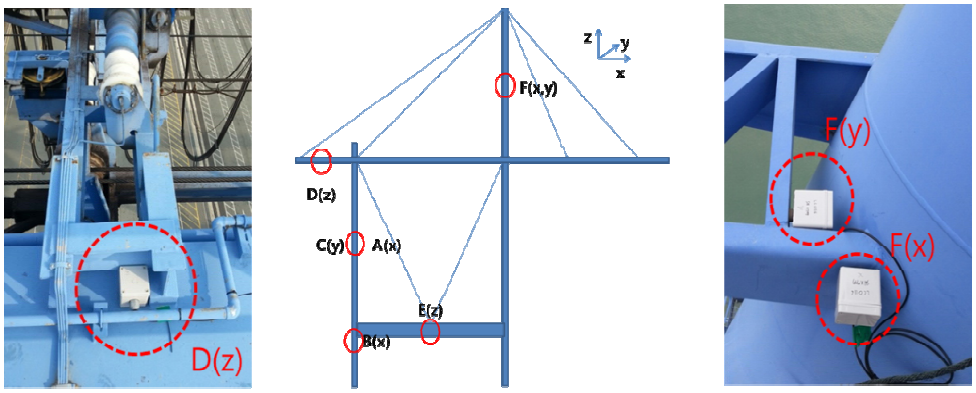

Fig. 2 Accelerometer locations and acceleration recording axes

for the safety design for the crane structures. For these reasons, using only one type of sensors to monitor the crane deformations is considered very complicated to extract the crane full periodic and identification movement models. However, this paper focuses on the analysis of the steel container crane at Pusan city port based on the accelerometer measurements under environmental loads and considering the container-moving load. Then using the FEM analysis and the identification model to study the safety and the vibration state of the crane in both time and frequency domains. Finally, assessing the crane behavior using the SHM system based on FEM analysis and results have been concluded.

2. Crane description and SHM system design

Container cranes are the typical portal structures, which are directly exposed to the typhoon, tsunami and earthquake. Especially, Pusan city ports are somewhat expected to be damaged by typhoons every year, and have experience of crane collapses in 2003 (Fig. 1). The crane condition diagnosis by SHM can give some useful preparation to natural disaster. In this study, real time monitoring system was built at a container crane located in Pusan city Newport. Target crane is made by ZPMC, which has 74 m height and 1,680 Ton weight. This model is most widely introduced and used in Korea ports, and which has representative nationally. Preliminary

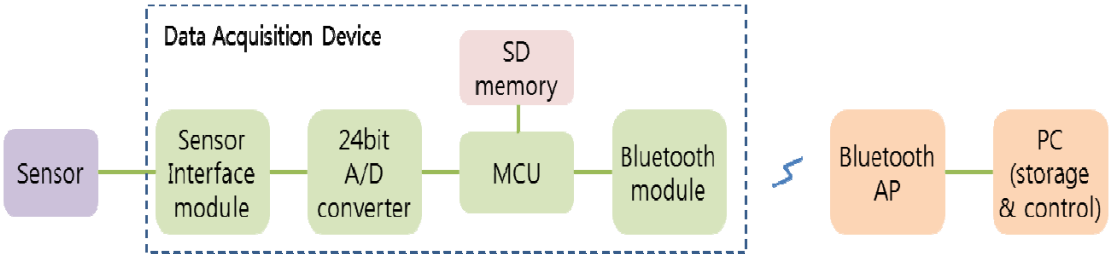

Fig. 3 Structural health monitoring system composition

Table 1 Acceleration sensor performance

Parameter	Description
Sensitivity (@160Hz)	10.046V/g
Amplitude	5g pk
Resolution	0.000002g rms
Transverse Sensitivity	3.9%
Frequency Range	0.1-300Hz (±10%)
Resonance Frequency	1.2kHz
Amplitude Linearity	<1%

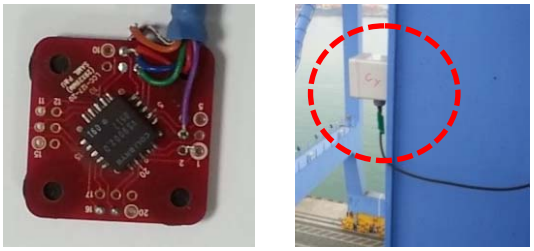

Fig. 4 Acceleration sensor photo, and in-situ installation at measuring point

simulation gave the measuring points for the accelerations monitoring (Fig. 2). Totally seven acceleration sensors were installed based on the FEM results.

SHM system of the container crane is composed (Fig. 3). Sensors are connected to a data acquisition device by wire. Measured data are digitized in AD converter and delivered through Bluetooth module and Access Point (AP) by wireless. The collected data are stored in SD memory and PC. A data acquisition device used in this research has one channel; each device was time synchronized by signal sender from PC each time. PC stores data in real time and controls the sensor nodes (data acquisition devices) (Table 2).

As a result of feasibility measurement, acceleration range of crane structure is about maximum 3g. Therefore, sensors were set which have the amplitude of 5g (Table 1 and Fig. 4). DAQ modules are prepared to measure the accelerations of each points of container crane. All devices are set inside the housing to protect against wind and rain (Fig. 5). The electric power was supplied from the crane machine room.

Table 2 Data-logger performance

Parameter	Description
Programmable Offset	~±5V
Transmit Frequency	2.0GHz Bluetooth
Sampling Rate	1~1000Hz
Synchronized Accuracy	10ms
Resolution	16bit
Size	80×80×32(mm)
Power saving	Wake/sleep
Data backup	Storage PC installed

Fig. 5 Experimental setting of data-loggers and storage PC

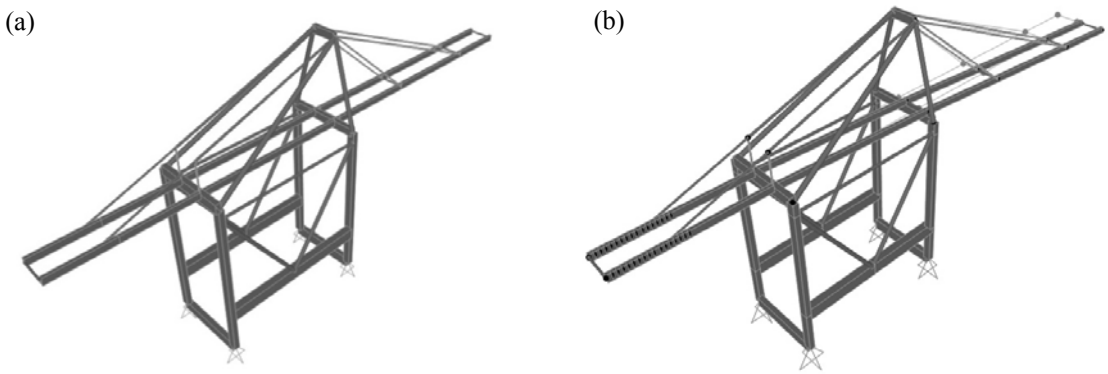

Fig. 6 (a) Crane finite element model and (b) first mode shape using SAP2000

3. Methodology

3.1 FEM design and load system

The Pusan crane is modeled using the SAP2000 software considering the dead load of the different steel members, the environmental conditions and the container-moving load (Fig. 6). The analyzed carne is a steel container crane that lifts objects by a hoist, which is fitted in a hoist trolley and move horizontally on pair of rails fitted under a beam. In addition, the steel material properties which are used in modeling the crane are presented in Table 3.

Table 3 Steel material properties

Density (ρ)	Modulus of Elasticity (E)	Poisson's ratio (v)	Shear Modulus (G)	Effective yield stress (Fye)	Effective tensile stress (Fue)
7850 kg/m^3	210000 N/mm^2	0.30	80000 N/mm^2	380 N/mm^2	500 N/mm^2

The crane consists of two main parts: the base and the moving load rail arm. The base width and depth are 42.67m and 20.60m, respectively. The second part is the moving load arm with total length 153.60m. During our experiments, both the container-moving load and environmental condition excited the crane. The moving load is a container with weight 65 Ton moving horizontally for a distance 127.67m along the crane arm with speed 1 m/sec on the main hoist. The FEM modal frequencies for the first five modes of the crane are 0.09; 0.398; 0.561; 0.657 and 0.659 Hz, respectively.

3.2 Identification model

In most practical applications, the system is not known and has to be estimated from the available information that is called the identification problem. The three main choices in system identification are data, model class and criterion. In addition, system identification often involves several runs of the empirical cycle that consists of the specification of the problem, the estimation of a model by optimization of the criterion, the validation of the resulting model, and possible adjustments that may follow from this validation. The method, which is used, is the multi input single output (MISO) Neural Network Auto-Regression model with eXogenous inputs (NNARX). In general, Auto-Regression eXternal input (ARX) model structure (Norgaard 2000, Zhiping *et al.* 2011) used delayed inputs and outputs in order to determine a prediction of the out-put at one (or more) sample interval(s) in the future. The most used model structure is the simple linear difference equation:

$$y(t) + a_1 y(t-1) + \cdots . + a_{na} y(t-na) = b_1 u(t-nk) + \cdots . + b_{nb} u(t-nk-nb+1 \quad (1)$$

Which relates the current output $y(t)$ to a finite number of past outputs $y(t-k)$ and inputs $u(t-k)$. The structure is thus entirely defined by the three integers na, nb, and nk. Where, na is equal to the number of poles and $nb-1$ is the number of zeros, while nk is the pure time-delay in the system. Parameter estimation of the linear ARX models is followed by a standard minimization of the sum squared errors approach (Norgaard 2000). In the absence of noise, the model could be determined directly from linear algebra from very few data points, in a relatively trivial manner. In the ARX structures, it is assumed that the noise is equivalent to pre-filtered white noise where the poles of the filter are identical to those of the resulting ARX model. Practically, this means that iteration may be necessary to ensure that deviation from this assumption does not have a deleterious effect on the model predictions (Norgaard 2000). In this paper, using Multilayer Perceptron (MLP) network to estimate the parameters and predict model output of Eq. (1). The MLP-networks considered here having only one hidden layer and only hyperbolic tangent and linear activation functions (f, F)

$$y_i(w, W) = F_i\left(\sum_{j=0}^{q} W_{ij} f_j\left(\sum_{l=1}^{m} w_{jl} z_l + w_{j0}\right) + W_{i0}\right) \quad (2)$$

Where, $y_i(w, W)$ is the prediction of the model as a function of network weights; w_{j0} and W_{i0}

are the bias parameters; m is the number of input units; and q is the number of hidden units. The function $f(.)$ that is implemented in this paper is a tangent function and $F(.)$ is a linear function output. The weights are the adjustable parameters of the network. z_l represents the feature vector of length m, presented to the input of a feed forward neural network. In this case, a feed-forward neural network is used with an input layer of m nodes for n=1…. m, one hidden layer and a single output layer. The input layer includes the input variables. The hidden layer consists of hidden neurons or units placed in parallel. Each neuron in the hidden layer performs a weighted summation of the weights which then passes an activation function. The output layer of the neural network is formed by another weighted summation of the outputs of the neurons in the hidden layer (Norgaard 2000). The purpose of the neural network learning process is to apply corrective adjustments to the synaptic weight of neuron in order to make the output to come closer to the desired response in a step-by-step manner to satisfy the minimum function loss and the Akaike's Final Prediction Error. Finally, the following neural network regression model is specified the training set by

$$\mathrm{Z^N} = \{[\mathrm{u(t), y(t)}]|\mathrm{t} = 1, \ldots \ldots \mathrm{N}\} \tag{3}$$

The objective of training is then to determine a mapping from the set of training data to the set of possible weights ($Z^N \rightarrow \hat{\theta}$) so that the network will produce predictions $\hat{y}(t)$, which in some sense are close to the true outputs $y(t)$. The Auto-Correlation Function (ACF) of the errors criteria can be used to evaluate and compare the quality of the model. The lag (m) Auto-Correlation (AC) is defined as

$$\lambda(\mathrm{m}) = \frac{1}{\mathrm{n}}\sum_{\mathrm{t=1}}^{\mathrm{n}} \mathrm{e(t-m)e(t)} \tag{4}$$

Herein, $e(t)$ is an error value between the observed and the predicted model values ($e(t)=y(t)-\hat{y}(t)$); the AC $\lambda(m)$ is zero when k is nonzero. A large AC when k is nonzero indicates that the error is not zero-mean white noise and implies that the model structure is not relevant to the model system or that there might be a need to increase the model order. In real applications, AC $\lambda(m)$ cannot be zero when m is nonzero because of limited length of observation points. In addition; the cross correlation between the prediction residuals and input parameters is applied to evaluate the effect of input parameters on the prediction output estimated by ARX model (Belmont and Hotchkiss 1997). If the value of AC and cross correlation falls within 95% of the confidence interval, the AC and cross correlation values are insignificant and this value equals zero (Norgaard 2000).

3.3 Statistical method

Structural analysis is required to determine whether significant movements occurred between the monitoring campaigns. Geometric modeling is used to analyze spatial displacements. Let us consider two sets of measurements in two epoch measurements ×1 and ×2 and it is needed to compare the two sets of directions and test the hypothesis that these are significantly different. The statistic test of the equality of the two mean directions is the F-statistic (Martin 2007).

$$\mathrm{F} = \left(1 + \frac{3}{8\mathrm{K}}\right)\frac{(\mathrm{n-2})(\mathrm{R_1+R_2-R_T})}{\mathrm{n-R_1-R_2}} \tag{5}$$

Where K is the concentration parameter, $R1$ and $R2$ are the resultant of epochs 1 and 2, respectively, and R_T is the resultant of the combined epochs. The concentration parameter can be

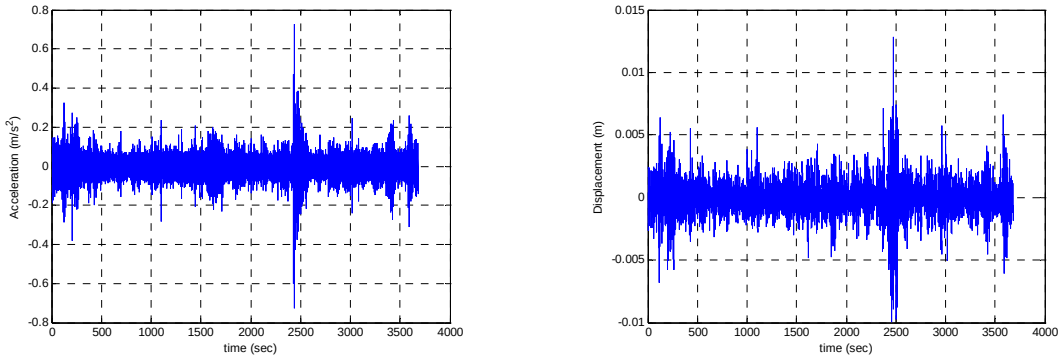

(a) (b)

Fig. 7 The acceleration and calculated displacement time histories of point A at 6:00am on February 21, 2013, (a) acceleration, (b) displacement

obtained from statistical tables using R_T (Martin 2007). The calculated F is compared with critical values from the standard F tables. The two mean directions are not significantly different if the measured F-value is lower than the critical F-value (from statistical tables), which depends on the degrees of freedom, and at significance level 5%.

4. Results and discussions

The crane oscillation amplitude and frequency with deformation model identification for the three selected points $A(X)$, $E(Z)$ and $F(X)$ can be described as follows:

4.1 Real time acceleration analysis

The real time acceleration analysis of the crane deformations in the time and frequency domains consist of the following steps:-

4.1.1 Dynamic displacement calculations

The acceleration measurements recorded on February 21, 2013 at points A, E and F are converted to the dynamic displacement as shown in Fig. 7. The dynamic displacement is calculated using double integration of the acceleration measurements after de-noising the observations and base correction (Meng *et al.* 2007). The mean relative dynamic displacements from the acceleration measurements at points A, F and E are presented as shown in Fig. 8. From Fig. 8, it can be shown that the maximum relative displacements are 8.15mm, 10.71mm and 5.74mm at points A, F and E, respectively. In addition, it can be shown that container-moving load period (crane working period) from 8.00 am to 16.00 pm on this day.

4.1.2 Static displacement calculations

From the FEM analysis that mentioned in section 3.1 and using the environmental input data shown in Fig. 9 and container-load conditions, the output displacements at the different observation points are investigated. The output displacement component in this case is considered

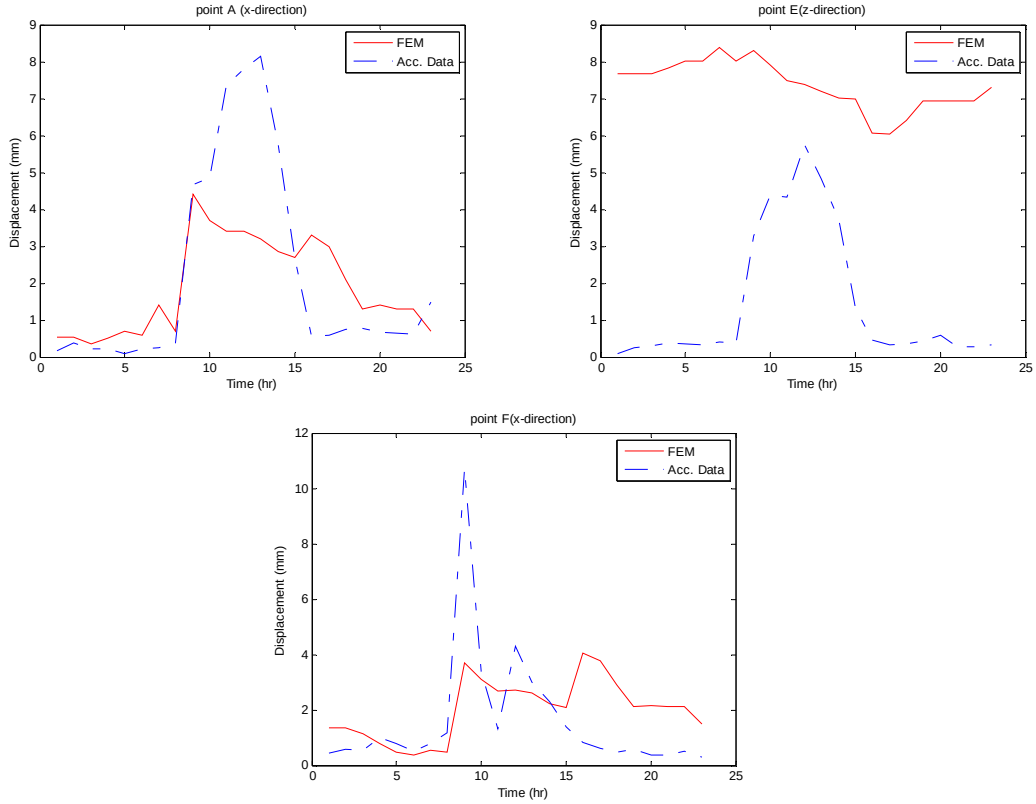

Fig. 8 Relative displacements of acceleration measurements and FEM for points *A*, *E* and *F* on February 21

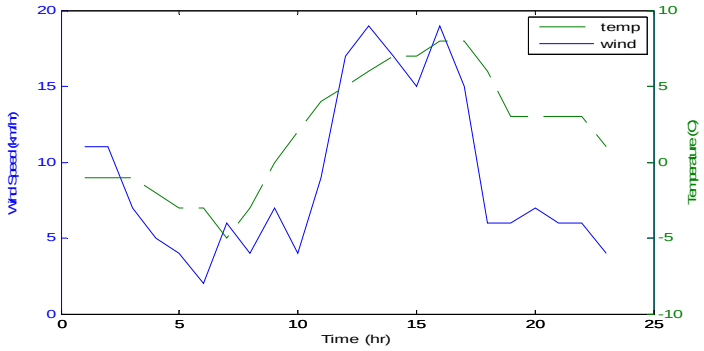

Fig. 9 Average wind speed and temperature on February 21, 2013

as a static component of the crane deformations as shown in Fig. 8. From Fig. 8, it can be shown that the maximum relative displacements are 4.40 mm, 3.70 mm and 8.30 mm at points *A*, *F* and *E*, respectively.

From the relative dynamic and static displacement components comparison, which presented in Fig. 8, it can be seen that the dynamic and static crane displacement components before and after

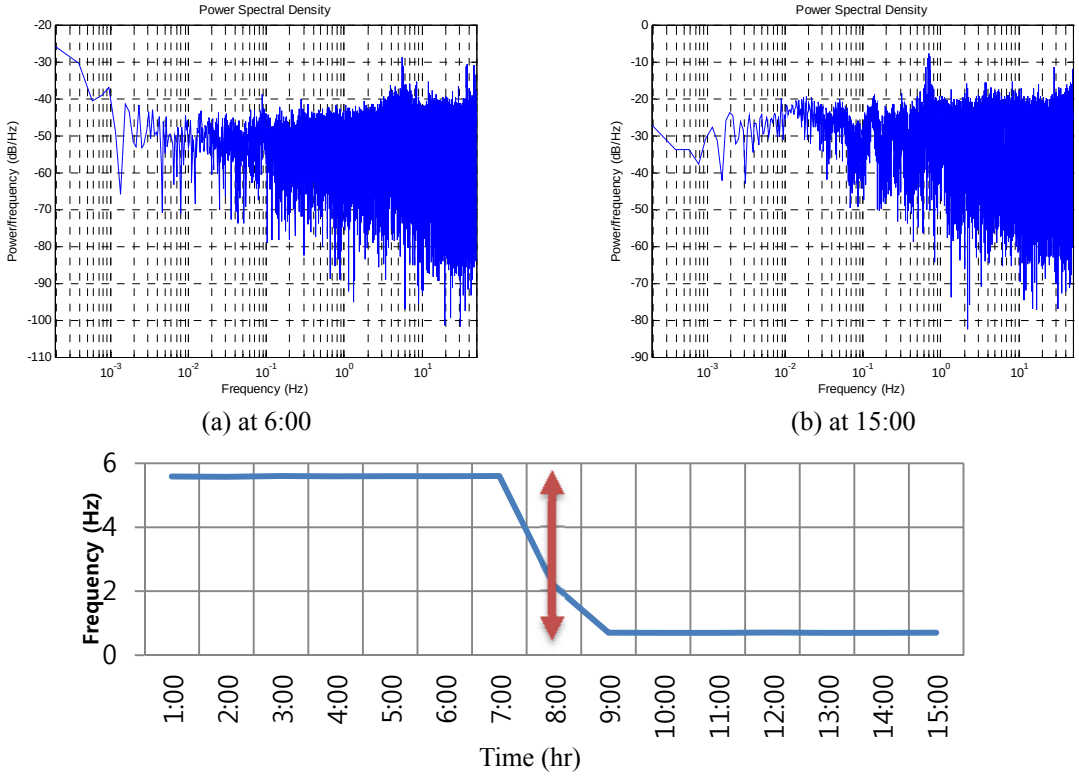

Fig. 10 The power spectra and fundamental frequencies of point A on February 21, 2013

the container-loading period are showing close values for points *A* and *F*. Otherwise, at point *E* the crane displacement components are not matching. This indicates that the rigidity of point E, which represents the connection point of the crane bracing members, affects the static displacement component calculated from the FEM. From these results, it can be concluded that the mean dynamic displacement, which calculated from acceleration measurements, cannot reveal the full crane displacement components under the container-loading case (Psimoulis *et al.* 2011). However, they can show the static movement of structures under the environmental load case, therefore, it is not easy to calculate the amplitude of the static displacements from acceleration measurements. In addition, the recording point's rigidity is affecting the static displacement components of the structure; therefore, the FEM cannot express the actual behavior of structures at these points.

4.1.3 Identification of oscillation frequency

The spectra of the dynamic components of the acceleration measurements corresponding to the crane loading cases were computed to investigate the existence of an oscillation signal and eventually detect the oscillation frequency. The Fast Fourier Transform (FFT) is used to calculate the first mode of the crane displacements as shown in Fig. 10. The power spectra of the acceleration observations of point A at two different observation hours in addition to the variation of the fundamental frequency of the acceleration observations of point A during all the observation hours are illustrated in Fig. 10. From this figure, it can be seen that the crane loading cases affect

Table 4 The fundamental frequencies of acceleration measurements and the FEM model at different points of the carne

Time (hr)	*A* (x-dir.)	*E* (z-dir.)	*F* (x-dir.)	FEM analysis	Load case
5:00 am	5.60 Hz	1.99 Hz	2.06 Hz	0.09 Hz	(ambient conditions)
11:00 am	0.70 Hz	13.48 Hz	0.70 Hz	0.18 Hz	(loading conditions)

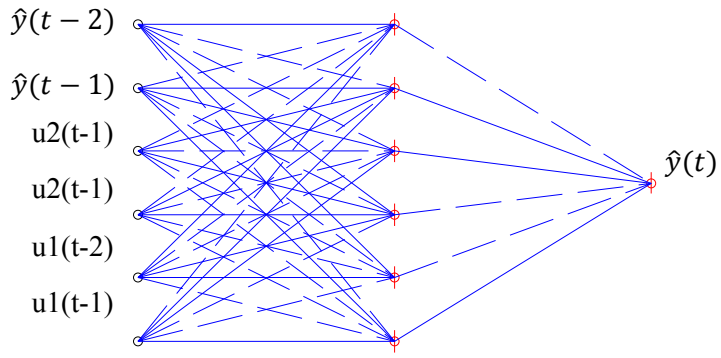

Fig. 11 NNARX [2 2 1] input, hidden and output neuron

the crane frequency mode. The drop in the first mode frequency of the acceleration measurements due to container moving load is 4.9 Hz, 11.49 Hz and 1.36 Hz at points *A*, *E* and *F*, respectively. From Fig. 10 and Table 4, it can be seen that the first mode frequencies of the crane is greater than first mode calculated from the FEM in the different loading conditions. Although, it can be shown that the rigidity of point E is affecting the first mode frequency of this point. From these results, it can be concluded that the crane displacements are within the safe limits under the different loading conditions, especially under the container-moving load case.

4.2 Model identification analysis

The Neural Network ARX model is used to identify the crane movements at points *E* and *F*. The model is design based on the acceleration measurements recorded at point *A* on February 21, 2013. The designed model based on multi-input single-output (MISO) to identify and to detect the crane movements under affected wind ($u1$) and temperature ($u2$) loads as shown in Figs. 9 and 11. For analyzing the NNARX model, initially fully connected network architecture with six hidden hyperbolic tangent units is selected. Two input delay for each input parameters and output prediction delay are used in this model NNARX [2 2 1], as shown in Fig. 11. This selection delay is used after testing the significance of the input and output number delay at level 5%. In addition, the purpose of the neural network learning process is to apply corrective adjustments to the synaptic weight of neuron in order to make the output to come closer to the desired response in a step-by-step manner to satisfy the minimum loss function; let the function initialize the weights, try maximum 1000 iteration and use a small weight decay between neural layers (Norgaard 2000).

From Figs. 12 (a) and (b), it can be seen that the NNARX [2 2 1] model is suitable to identify the crane movements of point *E*, whereas the *R*-Value about 0.95 and the maximum model error is 2.5 mm. Furthermore, it is suitable to identify the movement of point *F*, whereas the *R*-Value about

Table 5 Statistical movement of the crane points

Time (hr)	Point A	Point E	Point F
6:00-14:00	-1.4E-15	-4.62E-15	-4.43E-14
14:00-24:00	6.7E-16	-7.7E-15	-6.13E-15

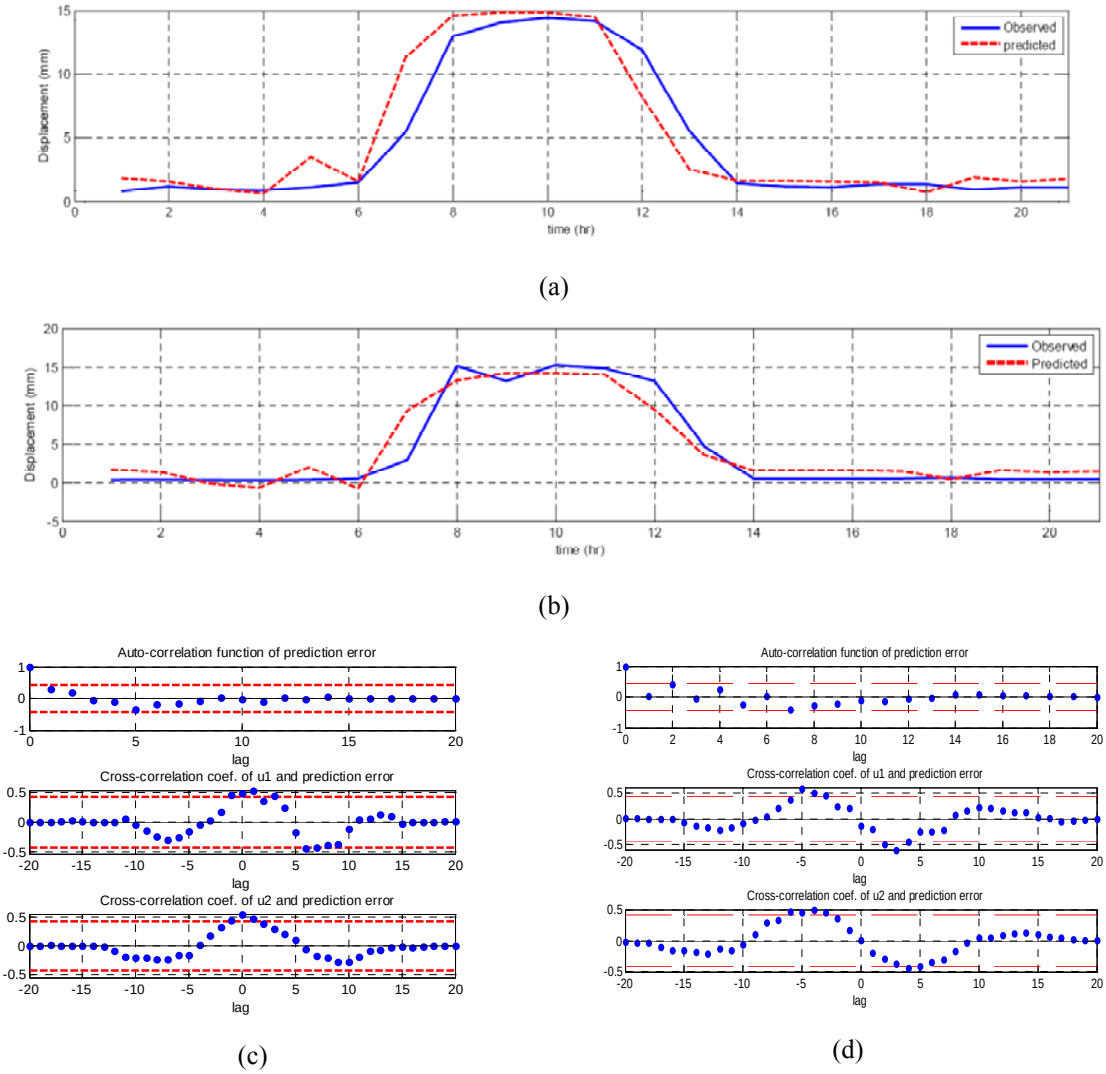

Fig. 12 (a), (b) model identification for points *E* and *F*; (c), (d) statistical model for points *E* and *F*, respectively

0.84 and the maximum model error is 4 mm. The autocorrelation function (ACF) of prediction errors and 95% confidence intervals and cross correlation coefficients of $u1$ and $u2$ with predicted errors and 95% confidence intervals were shown in Figs. 12 (c) and (d). From this Fig., it can be

show that no loss of information was observed since the residuals of this model stayed within confidence interval of the auto-correlation function and cross-correlation coefficients of $u1$ and $u2$. Herein, it can be concluded that the NNARX [2 2 1] model is reflecting the behavior of crane movements and can be used to detect the crane movements at different points of the crane. In addition, it can be also concluded that, the wind and temperature loads affect the crane movements in different cases of loading.

The statistical analysis of the crane movements at different points are calculated based on Eq. (5), as presented in Table 5. In this method, the original displacement data assume that the first measured displacement and the statistical analysis of the movements of the crane points are calculated in relative to this point. The F-value calculated in the three dimensions for the two points are less than the critical F-value (7.71) at level of significance is 0.05 (Table 5). Therefore, the movements of the crane points are not significant. Accordingly, it is concluded that the deformation and movement of the crane is very safe.

5. Conclusions

Based on the limited study of the container crane in Pusan city port, the analysis results lead to the following findings:

• The relative mean dynamic displacements of the crane are 8.15 mm, 10.71 mm and 5.74 mm at points A, F and E, respectively. While, the relative static displacements at points A, F and E are 4.40 mm, 3.70 mm and 8.30 mm, respectively.

• The mean dynamic displacements that are calculated from the acceleration measurements cannot reveal the full crane displacement and movement components in case of container-moving loads. However, they can show the static movement of structures under the environmental load case. Therefore, it is not easy to calculate the amplitude of the static displacements from the acceleration measurements.

• The rigidity of connections and members of structures affects the static displacement components of structures.

• The drops in the fundamental frequency values of the acceleration time histories due to the effect of container-moving loads are 4.9 Hz, 11.49 Hz and 1.36 Hz at points A, E and F, respectively. In addition, the fundamental frequency of the crane is greater than the FEM fundamental frequency in the two cases of loading. Furthermore, the rigidity of point E affects the fundamental frequencies of the acceleration measurements at this point.

• The NNARX [2 2 1] model reflects the behavior of the crane movements and can be used to detect the crane deformations at different locations on the crane.

• The crane movements are within the safe limits under the container-moving case of loading in both time and frequency domains and in the statistical movements analysis.

Acknowledgments

This research described in this paper was financially supported by the Ministry of Land, Transport and Maritime Affairs (MLTM) through a research project “Development of Infra Technology for 400km/h High Speed Rail”.

References

Belmont, M.R. and Hotchkiss, A.J. (1997), "Generalized cross-correlation functions for engineering applications, part i: basic theory", *J. Appl. Mech.*, **64**, 321-326.

Bhimani, A. and Soaderberg, E. (2010), "Quay crane accidents: lessons and prevention", Presentation TOC Asia 2010, Shanghai, China.

Chan, W.S., Xu, Y.L., Ding, X.L. and Dai, W.J. (2006), "An integrated GPS-accelerometer data processing technique for structural deformation monitoring", *Geodesy J.*, **80**, 705-719.

Deng, H. and Xu, J. (2009), "Construction safety monitoring and finite element analysis on the supporting system of tower crane in Guangzhou west-tower", *Proceeding of the Second International Conference on Information and Computing Science*, Manchester, England.

Ding, K.Q., Wang, Z., Lina, N. and Song, Q. (2012), "Structural health monitoring system for the crane based on bragg grating sensors", *Proceeding of 18th World Conference on Nondestructive Testing*, Durban, South Africa.

Elnabwy, M.T., Kaloop, M.R. and Elbeltagi, E. (2013), "Talkha steel highway bridge monitoring and movement identification using RTK-GPS technique", *Measurement J.*, **46**(10), 4282-4292.

Erdogan, H. and Gulal, E. (2009), "Identification of dynamic systems using multiple input-single output (MISO) models", *Nonlin. Anal., Real World Appl.*, **10**(2), 1183-1196.

Gentile, C. (2010), "Application of radar technology to deflection measurement and dynamic testing of bridges", Radar Technology, (Ed. Guy Kouemou), In Tech, 141-162.

Gevers, M., Miskovic, L., Bonvin, D. and Karimi, A. (2006), "Identification of multi-input systems: variance analysis and input design issues", *Automatica J.*, **42**(4), 559 – 572.

Gikas, V. (2012a), "Three-dimensional laser scanning for geometry documentation and construction management of highway tunnels during excavation", *Sensor. J.*, **12**(8), 11249-11270.

Gikas, V. (2012b), "Ambient vibration monitoring of slender structures by microwave interferometer remote sensing", *J. Appl. Geodesy*, **6**, 167-176.

Godoy, H.Y., Schoefs, F., Nouy, A. and Lasne, M. (2008), "Reliability analysis of two in-service monitored pile-supported wharves during extreme storm loading events", *Proceeding of 1st International Conference on Applications Heritage and Constructions in Coastal and Marine Environment*, Lisbon, Portugal.

Hart, G. and Yao, J. (1977), "System identification in structural dynamic", *J. Eng. Mech. Div.*, *ASME*, **103**(EM66), 1089-1104.

Heij, C. and Schagen, F. (2007), *Introduction to mathematical systems theory linear systems, identification and control*, Ed. Ran, A., Springer, Basel, Switzerland.

Heo, G. and Jeon, J. (2009), "A smart monitoring system based on ubiquitous computing technique for infra-structural system: centering on identification of dynamic characteristics of self-anchored suspension bridge", *KSCE Journal of Civil Engineering*, **13**(5), 333-337.

Kaloop, M.R. (2012), "Bridge safety monitoring based-GPS technique: case study Zhujiang Huangpu Bridge", *Smart Struct. Syst.*, **9**(6), 473-487.

Kaloop, M.R. and Li, H. (2014), "Multi input-single output models identification of tower bridge movements using GPS monitoring system", *Measurement J.*, **47**, 531- 539.

Kosbab, B., Jacobs, L., DesRoches, R., and Leon, R. (2009), "Analysis and testing of container cranes under earthquake loads", TCLEE 2009, 1-11, doi: 10.1061/41050(357)80.

Li, X., Ge, L., Ambikairajah, E., Rizos, C., Tamura, Y. and Yoshida, A. (2006), "Full-scale structural monitoring using an integrated GPS and accelerometer system", *GPS Solut. J.*, **10**, 233-247.

Magalhaes, F., Caetano, E. and Cunha, A. (2007), "Challenges in the application of stochastic modal identification methods to a cable-stayed bridge", *J. Bridge Eng.*, *ASCE*, **12**(6), 746-754.

Martin, H. (2007), *Matlab recipes for earth sciences*, 2th Edition, Springer Berlin Heidelberg, New York, USA.

Meng, X., Dodson, A.H. and Reborts, G.W. (2007), "Detecting bridge dynamics with GPS and triaxial accelerometers", *J. Eng. Struct.*, **29**(11), 3178-3184.

Moschas, F. and Stiros, S. (2011), "Measurement of the dynamic displacements and the modal frequencies of a short-span pedestrian bridge using GPS and an accelerometer", *J. Eng. Struct.*, **33**(1), 10-17.

Nickitopoulou, A., Protopsalti, K. and Stiros, S. (2006), "Monitoring dynamic and quasi-static deformations of large flexible engineering structures with GPS: accuracy, limitations and promises", *J. Eng. Struct.*, **28**(10), 1471-1482.

Norgaard, M. (2000), "Neural network based system identification toolbox", Version2. Tech. Report, 00-E-891, Department of Automation, Technical Un. of Denmark.

Psimoulis, P., Moschas, F. and Stiros, S. (2011), "Measuring the displacements of a rigid footbridge using geodetic instruments and an accelerometer", *Proceeding of JUSDM*, Hong Kong, China.

Richard, L.N., Seixas, N.S. and Ren, K. (2001), "A review of crane safety in the construction industry", *Appl. Occup. Environ. Hyg. J.*, **16**(12), 1106-1117.

Sohn, H., Farrar, C.R., Hemez, F.M., Shunk, D., Stinemates, D.W., Nadler, B.R. and Czarnecki, J.J. (2004), "A review of structural health monitoring literature: 1996–2001", Los Alamos National Laboratory Report, LA-13976-MS.

Weng, J., Loh, C., Lynch, J., Lu, K, Lin, P. and Wang, Y. (2008), "Output-only modal identification of a cable-stayed bridge using wireless monitoring systems", *J. Eng. Struct.*, **30**, 1820-1830.

Zhiping, L., Tengfei, J., Qing, H. and Dang, W. (2011), "Research on mechanical condition monitoring technology for portal crane by wireless sensors", *Proceeding of 3rd International Conference on Measuring Technology and Mechatronics Automation*, Shanghai, China.